

Ligand-dependent interactions between SR-B1 and S1PR1 in macrophages and atherosclerotic plaques

Christine Bassila, George E. G. Kluck, Narmadaa Thyagarajan, Kevin M. Chathely, Leticia Gonzalez[✉], and Bernardo L. Trigatti^{*✉}

Department of Biochemistry and Biomedical Sciences, Thrombosis and Atherosclerosis Research Institute, Hamilton Health Sciences, McMaster University, Hamilton, ON, Canada

Abstract HDLs carry sphingosine-1-phosphate (SIP) and stimulate signaling pathways in different cells including macrophages and endothelial cells, involved in atherosclerotic plaque development. HDL signaling via SIP relies on the HDL receptor scavenger receptor class B, type I (SR-B1) and the sphingosine-1-phosphate receptor 1 (S1PR1), which interact when both are heterologously overexpressed in the HEK293 cell line. In this study, we set out to test if SR-B1 and S1PR1 interacted in primary murine macrophages in culture and atherosclerotic plaques. We used knock-in mice that endogenously expressed S1PR1 tagged with eGFP (*S1pr1^{eGFP/eGFP}* mice), combined with proximity ligation analysis to demonstrate that HDL stimulates the physical interaction between SR-B1 and S1PR1 in primary macrophages, that this is dependent on HDL-associated SIP and can be blocked by an inhibitor of SR-B1's lipid transfer activity or an antagonist of S1PR1. We also demonstrate that a synthetic S1PR1-selective agonist, SEW2871, stimulates the interaction between SR-B1 and S1PR1 and that this was also blocked by an inhibitor of SR-B1's lipid transport activity. Furthermore, we detected abundant SR-B1/S1PR1 complexes in atherosclerotic plaques of *S1pr1^{eGFP/eGFP}* mice that also lacked apolipoprotein E. Treatment of mice with the S1PR1 antagonist, Ex26, for 12 h disrupted the SR-B1-S1PR1 interaction in atherosclerotic plaques. **■** These findings demonstrate that SR-B1 and S1PR1 form ligand-dependent complexes both in cultured primary macrophages and within atherosclerotic plaques in mice and provide mechanistic insight into how SR-B1 and S1PR1 participate in mediating HDL signaling to activate atheroprotective responses in macrophages.

Supplementary key words atherosclerosis • high-density lipoprotein • macrophage • scavenger receptor class B type I • sphingosine-1-phosphate • sphingosine-1-phosphate receptor 1

Atherosclerosis is a leading cause of ischemic cardiac, cerebrovascular, and peripheral arterial disease and a major contributor to disease and death globally (1). It is a progressive inflammatory disease initiated with the

subendothelial retention, in the intima of artery walls, of apolipoprotein B (apoB)-containing lipoproteins and their subsequent oxidation (2). Oxidized LDL (ox-LDL) activates innate immune cells, particularly monocyte-derived macrophages, which engulf the ox-LDL through their constitutively expressed scavenger receptors on the cell surface (3). Although macrophages effectively clear ox-LDL, it is cytotoxic and can induce macrophage apoptosis as well as necroptosis (4–7). However, impaired macrophage-mediated efferocytosis (binding and clearance of apoptotic cells) in atherosclerotic plaques results in the persistence of apoptotic cell debris and secondary necrosis, which combined with ongoing necroptosis leads to the release of cell-derived cholesterol, proteases, and cellular-derived damage-associated molecular patterns acting as inflammatory mediators, to drive atherosclerotic plaque development (8, 9).

Numerous epidemiological and preclinical studies have demonstrated that HDL protects against atherosclerosis (10–14). This has long been attributed to its role in reverse cholesterol transport, a process through which cell cholesterol is taken up by HDL from peripheral cells (including foam cells) and is delivered to the liver for excretion into bile or for recycling back into the bloodstream (15–17). Hepatic uptake of HDL-cholesterol is mediated by the scavenger receptor class B type I (SR-B1), an HDL receptor that is encoded by the *SCARB1* gene (18, 19). SR-B1 is a 509 amino acid transmembrane glycoprotein, composed of two hydrophobic transmembrane domains and two relatively short cytoplasmic domains at the N and C termini (15, 20). Its extracellular domain contains a hydrophobic channel extending from the HDL-binding site to the cell plasma membrane, allowing the efficient bidirectional movement of cholesterol between bound HDL and cells (21–26).

HDL also mediates a variety of other antiatherogenic effects including the induction of intracellular

*For correspondence: Bernardo L. Trigatti, trigatt@mcmaster.ca.

signaling pathways in macrophages, endothelial, and smooth muscle cells (5, 6, 27–38). Many of these effects are mediated by the HDL-associated bioactive lysosphingolipid, sphingosine-1-phosphate (SIP) (28, 30–33, 37, 39, 40). SIP is generated by the phosphorylation of sphingosine, catalyzed by sphingosine kinases 1 and 2 and irreversibly degraded to phosphoethanolamine and hexadecanal by SIP-lyase (SIPL) (41). Most (65–98%) of the plasma SIP is associated with HDL (42, 43) through binding to a hydrophobic ligand-binding pocket of apo M, associated with a subset of HDL particles (44). SIP mediates a wide spectrum of cellular functions in different types of cells by binding to five related G-protein-coupled receptors, named SIP Receptors (SIPR) 1–5 (45). SIPR1, SIPR2, and SIPR3 are ubiquitously expressed, whereas SIPR4 is primarily expressed in lymphoid tissues and SIPR5 is found almost exclusively in the brain and spleen (46, 47).

We have previously reported that HDL treatment of macrophages in culture stimulates their migration and protects them against apoptosis and necroptosis induced by a variety of stimuli (5, 6, 28, 30). We demonstrated that HDL signaling in macrophages requires SR-BI, which acts as an HDL receptor, an adaptor protein, postsynaptic density protein/drosophila disc-large protein/zonula occludens protein containing 1 (PDZK1), which reportedly binds to the cytoplasmic carboxy terminus of SR-BI and SIPR1 resulting in Akt 1 phosphorylation (5, 6, 28, 30). On the other hand, HDL-mediated signal transducer and activator of transcription 3 activation in macrophages involves SIPR2 and SIPR3 (35). HDL signaling in endothelial cells also involves SR-BI, both SIPR1 and SIPR3 and HDL-associated SIP (37). Conditional inactivation of *Sipr1* gene expression either in myeloid or endothelial cells increases atherosclerosis in mice (30, 32). Similarly, genetic inactivation of either *Sr-b1* or *Pdzk1* in bone marrow-derived cells increases atherosclerosis in mice, and knockout of either *Sipr1*, *Sr-b1*, or *Pdzk1* in bone marrow-derived/myeloid cells increases apoptosis and necrotic core development within atherosclerotic plaques (5, 30, 48), consistent with the possibility that these three factors participate in the same pathway.

Others have previously reported that when overexpressed in transfected HEK293 cells, SR-BI and SIPR1 proteins form complexes in the presence of HDL-bound SIP (49). This may explain the functional requirement of both SR-BI and SIPR1 for HDL signaling that has been reported in macrophages (5, 28, 30) and endothelial cells (37). However, whether SR-BI and SIPR1 form complexes at physiological levels of endogenous expression in macrophages either in culture or within atherosclerotic plaques has not been tested.

Therefore, we sought to examine if SR-BI and SIPR1 receptors might interact physically under more physiologically relevant conditions of endogenous expression levels in primary macrophages and in

atherosclerotic plaques in mice. We demonstrate that SR-BI and SIPR1 interact in an HDL-dependent manner in peritoneal macrophages and in cells within atherosclerotic plaques from *ApoE*-deficient mice. We report that this HDL-stimulated interaction depends on HDL-associated SIP, SR-BI's lipid transfer activity, and SIPR1 activity.

MATERIALS AND METHODS

Mice

All procedures involving experimental mice were first approved by the McMaster University Animal Research Ethics Board and were in accordance with the Canadian Council of Animal Care guidelines. Mice were bred and group housed at the David Braley Research Institute animal facility under controlled temperature and light and provided with free access to automatic watering and standard chow diet. All mice were on a C57BL/6J background. *Sr-b1*^{KO/KO} mice were derived from founders originally obtained from Professor Monty Krieger (Massachusetts Institute of Technology) and backcrossed >10 generations to C57BL/6J mice (50). C57BL/6J wild-type, *ApoE*^{KO/KO}, and SIPR1-enhanced green fluorescent protein (eGFP) knock-in mice (referred to as *Sipr1*^{eGFP/eGFP} in which eGFP was inserted in the coding sequence of the *Sipr1* gene, leading to the expression of a fully functional SIPR1-eGFP fusion protein (51)) were each bred from founders originally purchased from Jackson Laboratories (Bar Harbor, ME). *Sipr1*^{eGFP/eGFP}/*ApoE*^{KO/KO} mice were generated by breeding *Sipr1*^{eGFP/eGFP} mice to *ApoE*^{KO/KO} mice. The double heterozygous offspring were each intercrossed to generate double-homozygous mice, which were then bred to generate the mice used for experiments.

Cell preparation culture and treatment

Peritoneal macrophages were elicited by intraperitoneal injection of 1 ml of 10% thioglycolate (Millipore Sigma Canada, Oakville, ON, Canada). At day 4 post-injection, mice were anesthetized with isoflurane and then euthanized by CO₂ asphyxiation and cervical dislocation. Macrophages were collected by peritoneal lavage using 10 ml of PBS containing 5 mM of EDTA, then centrifuged at 1,200 *g* for 5 min, and resuspended in DMEM supplemented with 10% FBS, 2 mM L-glutamine, 50 µg/ml penicillin, and 50 U/ml streptomycin. Macrophages were counted by hemocytometer and plated in either 8-well chambered slides at 0.7 × 10⁵ cells per 0.8 cm² well for Duolink in situ proximity ligation assay (PLA) or in 6-well culture plate at 2 × 10⁶ cells per 9.5 cm² well for immunoblotting. Cells were then cultured at 37°C in an atmosphere of 5% CO₂ in air for 2 h allowing macrophages to adhere. Macrophages were then washed at least two times with 1× PBS and incubated for 16 h in DMEM containing 10% FBS, 2 mM L-glutamine, 50 µg/ml penicillin, and 50 U/ml streptomycin.

For Duolink in situ PLA, macrophages were incubated with DMEM supplemented with 3% newborn calf lipoprotein-deficient serum, 2 mM L-glutamine, 50 µg/ml penicillin, and 50 U/ml streptomycin, for 16 h prior to treatment. On the next day, cells were pre-treated for 45 min or 1 h at 37°C with immunological or pharmacological inhibitors followed by HDL addition to macrophages for 30 min. For some experiments, HDL was first pre-treated with recombinant active

human SIPL (0.02 µg/1 mg of HDL protein; Millipore Sigma Canada, Oakville, ON, Canada; catalog # SRP0191) or vehicle for 1 h at 37°C before adding it to the cells for 30 min. In other experiments, cells were pre-treated for 45 min with SR-B1 blocking antibody or BLT-1 before adding the HDL and incubation for an additional 30 min. The following compounds were used: anti-SR-B1 blocking antibody, KKB-1, 1.5 µg/ml; originally generated by Karen Kozarsky, SwanBio Therapeutics and provided by Monty Krieger, Massachusetts Institute of Technology) (52); BLT-1 (150 nM, Millipore Sigma Canada, Oakville, ON, Canada; catalog #SML0059); SIP (10 nM, Avanti Polar Lipids, Inc, Birmingham AL; catalog # 860492P); HDL (100 µg/ml; Athens Research And Technology, Athens, GA; catalog #12-16-080412); SEW2871 (1 µM, Cayman Chemicals, Ann Arbor, MI; catalog #10006440), and Ex26 (10 µM, Tocris Bioscience, Bio-Techne Canada, Toronto, ON, Canada; catalog #5833/10). Control cells were treated with corresponding dilutions of solvent/vehicle. Immediately after treatment, macrophages in 8-well chambered slides were washed twice with 1x PBS. The cells were then fixed with 4% paraformaldehyde (PFA) diluted in 1x PBS for 20 min at room temperature (RT), washed three times with 1x PBS, and then Duolink in situ PLA was performed (as described below).

HDL analysis

HDL that was treated with SIPL or vehicle for 1 h at 37°C, as described above, was fractionated by gel filtration fast-protein liquid chromatography using an AKTA system with a Tricorn Superose 6 HR10/300 column and in line UV absorbance detector (GE Healthcare Life Sciences, Baie D'Urfe, QC, Canada) and 100 µl fractions were collected. Cholesterol levels on each fraction were analyzed by the Infinity Cholesterol enzymatic assay kit (Thermo Fisher Scientific, Ottawa, ON, Canada; catalog #TR13421) to measure total cholesterol. Afterward, the fractions corresponding to the cholesterol peaks were pooled by sets of five fractions starting from fraction 27 to fraction 51. This was done by taking 2.1 µl from each fraction. These five pools of fractions (10 µl of each pool) were subjected to SDS-PAGE immunoblotting with either goat anti-human ApoA1 antiserum (Midland Bio-products, Nittobo America Inc, Murrieta CA; catalog #71107) or mouse monoclonal anti-ApoM (8F12) antibody (Cell Signaling Technology, Danvers, MA; catalog #5709) and detection was carried out as described below.

Immunoblotting

Macrophages were washed twice with 1x PBS and then lysed with ice cold RIPA buffer (50 mM Tris-HCl pH-7.4; 150 mM NaCl; 1% Triton X-100; 1% sodium deoxycholate; 0.1% SDS; 1 mM EDTA) supplemented with protease inhibitors containing 1 mM phenylmethylsulfonyl fluoride (Thermo Fisher Scientific, Ottawa, ON, Canada; catalog #36978), 1 µg/ml pepstatin A, 1 mg/ml leupeptin, and 2 µg/ml aprotinin (Millipore Sigma, Canada, Oakville, ON, Canada; catalogs # P5318, L2884, and A1153). Cell lysates were centrifuged for 20 min at 12,000 g. Protein concentration was determined from supernatants using the Pierce BCA protein assay kit (Thermo Fisher Scientific, Ottawa, ON, Canada). Afterward, 30 µg protein per lane were mixed with Invitrogen Novex NuPAGE LDS Sample Buffer 4x (Thermo Fisher Scientific, Ottawa, ON, Canada; catalog # NP0007) and incubated at RT for 25 min and immediately subjected to PAGE and immunoblotting. PAGE was carried out using precast NuPAGE 4–12% Bis-Tris gradient gels (Thermo Fisher Scientific, Ottawa, ON, Canada; catalog # NP0321BOX)

with 1x MOPS SDS running buffer according to the manufacturer's instructions. Gels were then electrophoretically transferred to a polyvinylidene fluoride membrane, using a transfer buffer containing 480 mM of Tris, 390 mM of glycine, and 0.375% SDS, at 250 mA for 90 min at 4°C. Membranes were blocked with 5% BSA (New England Biolabs Canada, Whitby, ON, Canada; catalog # 9998S) diluted in TBS containing 0.1% Tween-20 for 1 h at RT. The following antibodies were then used: rabbit anti-SR-B1 (NB400-104; Novus Biologicals), Goat anti-GFP (Abcam Inc, Boston, MA; catalog # ab6673), and HRP-conjugated rabbit anti-β-Actin (Cell Signaling Technology, Danvers, MA; catalog # 5125S). After overnight incubation at 4°C, membranes were washed and incubated with either HRP-donkey anti-rabbit IgG (Jackson ImmunoResearch Laboratories, West Grove, PA; catalog #711-035-152), HRP-rabbit anti-goat IgG (Jackson ImmunoResearch Laboratories, West Grove, PA; catalog # 305-035-003), or HRP-donkey anti-mouse IgG (Jackson ImmunoResearch Laboratories, West Grove, PA; catalog #715-035-150) at 1:5,000 dilution for 1 h at RT. HRP was detected using the Pierce Enhanced Chemiluminescence Western Blotting Substrate (Thermo Fisher Scientific, Ottawa, ON, Canada; catalog # 32106) and a ChemiDoc imaging system (Bio-Rad Laboratories, Hercules, CA).

Atherosclerosis analysis

We fed *ApoE*^{KO/KO} and *S1pr1*^{eGFP/eGFP}/*ApoE*^{KO/KO} mice a high-fat diet (21% butter fat and 0.15% cholesterol, Dyets Inc, Bethlehem PA; catalog #112286), beginning at 15 weeks of age, for eight weeks. Twelve hours before harvest, *S1pr1*^{eGFP/eGFP}/*ApoE*^{KO/KO} mice received intraperitoneal injections of Ex26 (30 mg/kg; n = 4 per group) dissolved in dimethyl sulfoxide (DMSO). Control mice received only DMSO vehicle control (n = 4). Mice were simultaneously fasted for 12 h prior to undergoing isoflurane anesthesia and euthanasia. Hearts were perfused through the left ventricle with 0.9% NaCl containing 10 U of heparin/ml. Hearts were then harvested and frozen in Shandon Cryomatrix embedding medium (Thermo Fisher Scientific, Ottawa, ON, Canada) and stored at -80°C for further analysis. Atherosclerotic plaques from serial cross-sections (10 µm thickness) of the aortic sinuses were stained with oil red O and counterstained with Meyer's Hematoxylin solution as previously described (5, 6, 30). The cryosections were mounted with CLEAR-MOUNT (BioMeda Corporation, CA; catalog #17985-15). Images were obtained using a Zeiss Axiovert 200 M microscope (Carl Zeiss Canada Ltd Toronto, ON, Canada) at 5x magnification.

Proximity ligation assay

PLA was performed using Duolink In Situ Detection Reagents Red kit (Millipore Sigma Canada, Oakville ON, Canada; catalog #DUO92008) to examine interactions of endogenous SR-B1 and SIP1-GFP in primary peritoneal macrophages from *S1pr1*^{eGFP/eGFP} knock-in mice and sections of atherosclerotic plaques from *S1pr1*^{eGFP/eGFP}/*ApoE*^{KO/KO} mice. Cultured cells and histological sections were first fixed with 4% PFA as described above. When macrophages were co-stained with Alexa-488 conjugated wheat germ agglutinin (WGA; Thermo Fisher Scientific, Ottawa ON, Canada; catalog # W11261), they were first washed 3x with TBS for 3 min, blocked with 2% BSA in TBS for 20 min, washed 3x with TBS for 3 min, incubated with Alexa 488-WGA diluted 1:500 in 2% BSA in TBS for 15 min, and washed 2x with TBS for 2 min. At this point, WGA-stained cells as well as unstained macrophages and histological sections were permeabilized on ice for 10 min

with 0.1% Triton X-100. Samples were then blocked with Duolink® Blocking Solution in a heated humidity chamber for 1 h at 37°C. Afterward, the slides were incubated overnight at 4°C with the following primary antibodies: a goat polyclonal anti-GFP antibody (1:100; Abcam Inc Boston MA; catalog # ab6673) and a rabbit polyclonal anti-SR-BI antibody (1:100; Bio-Techne Canada, Toronto ON, Canada; catalog # NB400-104), and for some experiments, when cells or histological sections were co-stained for either caveolin-1 or Mac3, respectively, with a mouse monoclonal anti-caveolin 1 (1:500; Bio-Techne Canada, Toronto ON, Canada; catalog # NBP3-23193) or a mouse monoclonal anti-Mac3 antibody (1:200; BD Biosciences; catalog # 553322). Afterward, samples were washed three times with Duolink® wash buffer A (10 mM Tris, pH-7.4, 150 mM NaCl, and 0.05% Tween; Millipore Sigma Canada, Oakville ON, Canada; catalog # DUO82047) under gentle agitation. Anti-rabbit MINUS (Millipore Sigma Canada, Oakville ON, Canada; catalog # DUO92005) and anti-goat PLUS (Millipore Sigma Canada, Oakville ON, Canada; catalog #DUO92003) oligonucleotide-labeled secondary antibodies were added. After 1 h of incubation at 37°C, the slides were washed three times with Duolink® wash buffer A at RT. Slides were then incubated for 30 min at 37°C with the Duolink® ligation mix prepared by diluting 5× Duolink® Ligation buffer (1:5) and ligase (1:40) in water, followed by three washes with Duolink® wash buffer A. Next, the slides were incubated for 100 min at 37°C with the amplification solution prepared by diluting 5× Duolink® Amplification buffer (1:5) and rolling circle polymerase (1:80) in water. For experiments in which cells or tissue sections were co-stained for caveolin-1 or Mac3, respectively, slides were incubated with Alexa488-labeled goat anti-mouse secondary antibody (Thermo Fisher Scientific Canada, Ottawa, ON, Canada; catalog # A21042) for 1 h at room temperature. The slides were then washed two times with Duolink® Wash Buffer B (200 mM Tris, pH-7.5, 100 mM NaCl; Millipore Sigma Canada, Oakville ON, Canada; catalog # DUO82048) and one time with 0.01× Duolink® Wash Buffer B. Finally, the slides were mounted with Duolink® PLA Mounting Medium with DAPI (Millipore Sigma Canada, Oakville ON, Canada; catalog #DUO82040) for 15 min at RT and imaged using Stellaris 5 Confocal Microscope from Leica Microsystems with either a 20× or 63× objective for cells and 63× objective for histological sections of atherosclerotic plaques. For quantification of PLA staining in cultured cells, 3–5 20× fields of view were captured, while for atherosclerotic plaques, 3 63× fields of view were captured for atherosclerotic plaques from each of three sections per mouse. Images were analyzed using ImageJ software. For analyses of PLA staining, images of the red (PLA) and blue (DAPI) channels were each converted to 8 bit format and thresholds were set using the ImageJ “Threshold” function to eliminate background noise. Parameters such as size and circularity of particles were set using the “Analyze Particles” function of ImageJ to specify the characteristics of the particles included in the analysis. For quantification of cells stained for PLA and DAPI and imaged at 20× magnification, each particle identified in the PLA channel corresponded to a cell positive for PLA staining and each particle identified in the DAPI channel corresponded to a nucleus. The number of PLA-positive cells across the 3–5 fields of view were divided by the number of DAPI-stained nuclei across the same number of fields of view to obtain a percentage of the cells that were positive for PLA staining. For quantification of PLA staining in atherosclerotic plaques imaged at 63× magnification, particles identified from the PLA channel corresponded to foci of PLA staining in cells. The extent of

PLA staining was therefore expressed as the numbers of foci of PLA staining across three fields of view divided by the numbers of DAPI-stained nuclei in the same three fields of view to obtain the number of PLA staining foci per cell.

Cholesterol efflux

Thioglycolate-elicited peritoneal macrophages were collected from wild-type C57BL/6J mice, cultured in 96-well plates in RPMI containing 10% FBS, 2 mM L-glutamine, 50 µg/ml penicillin, and 50 U/ml streptomycin, for 16 h before changing the medium to phenol red-free RPMI containing 3% newborn calf lipoprotein-deficient serum, 2 mM L-glutamine, 50 µg/ml penicillin, and 50 U/ml streptomycin and culturing for an additional 16 h as described above. Following the manufacturer's instructions, cholesterol efflux was measured using the cell-based fluorescent Cholesterol Efflux Assay kit (Abcam Inc, Boston MA; catalog # ab196985). Cells were preloaded with the fluorescent tracer for 1 h, after which the loading solution was removed, cells were washed, and efflux was initiated by adding the efflux acceptor. Efflux was monitored using either no acceptor, untreated HDL, SIPL-treated HDL, or control-treated HDL (all at 100 µg protein/ml) as cholesterol acceptors. Some cells were also treated with Ex26 (10 µM) or BLT-1 (150 nM) during efflux. In addition, blank wells containing incubation medium without fluorescent cholesterol labeling reagent were included as controls. At the end of 3 h, media was collected, cells were lysed, and fluorescence (excitation 485 nm/emission 523 nm) was determined in each using a SpectraMax 3 fluorescence plate reader. The fluorescence of media from unloaded wells was subtracted from the fluorescence of media from cells loaded with the fluorescent cholesterol tracer to account for the intrinsic background fluorescence of the media. The percentage of cholesterol efflux was calculated as the ratio between the corrected RFU of the media to the sum of the corrected RFU of the media + RFU of the cell lysate × 100%.

Apoptosis

Thioglycolate-elicited peritoneal macrophages were collected from wild type C57BL/6J mice, cultured in eight well chamber slides in DMEM containing 10% FBS, 2 mM L-glutamine, 50 µg/ml penicillin, and 50 U/ml streptomycin, for 16 h prior to changing the medium to DMEM containing 3% newborn calf lipoprotein-deficient serum, 2 mM L-glutamine, 50 µg/ml penicillin, and 50 U/ml streptomycin, for an additional 16 h as described above. Cells were then cultured for 24 h in the absence or presence of tunicamycin (10 µg/ml), HDL (50 µg protein/ml), BLT-1 (150 nM), or combinations of those as described. Alternatively, cells were incubated in the absence or presence of tunicamycin and either SIPL-treated or control-treated HDL (as described above). After 24 h, cells were fixed in 4% PFA in PBS for 15 min at room temperature, washed with PBS twice, and subjected to Terminal deoxynucleotidyl transferase-mediated dUTP Nick End Labeling (TUNEL) using the ApopTag® Fluorescein In Situ Apoptosis Detection Kit (Millipore Sigma Canada, Oakville, ON, Canada; catalog #S7110) following the manufacturer's instructions. Slides were washed in PBS and counterstained with DAPI (300 nM) for 5 min. The slides were then washed and mounted with microscope slide cover glass by using PermaFluor™ aqueous mounting medium (Thermo Fisher Scientific, Ottawa, ON, Canada; catalog # TA-030-FM). After mounting the slides, they were imaged using a Zeiss Axiovert 200 M inverted fluorescence microscope (Carl Zeiss Canada

Ltd. Toronto, ON, Canada) using a 40× objective. Four fields were imaged from each well and the total number of TUNEL-positive nuclei were counted across the four fields and divided by the total number of nuclei as detected by DAPI to determine the % TUNEL-positive cells in each well.

Statistical analysis

Data was analyzed utilizing GraphPad Prism 6 software (San Diego, CA). Nonparametric Kruskal-Wallis ANOVA test for multiple groups was used. Data were presented as mean ± SEM and were considered statistically significant when $P < 0.05$.

RESULTS

HDL stimulates the interaction between SR-BI and SIPRI-eGFP in macrophages

To examine if SR-BI and SIPRI, expressed at endogenous levels in murine macrophages, physically interact with each other in an HDL dependent-manner,

we made use of $S1pr1^{eGFP/eGFP}$ mice in which *eGFP* was knocked in-frame into the *S1pr1* gene generating an SIPRI-eGFP fusion protein expressed at endogenous SIPRI levels (51). This allowed us to use eGFP as a C-terminal epitope tag for the SIPRI-eGFP fusion protein. SR-BI was detected by immunoblotting using an antibody against the C-terminal cytoplasmic tail of SR-BI in extracts from macrophages from C57BL/6J ($Sr-b1^{WT/WT}$) but not $Sr-b1^{KO/KO}$ mice (Fig. 1A). Likewise, using an antibody against the eGFP tag of SIPRI-eGFP, it was detected by immunoblotting in the extracts of primary macrophages from $S1pr1^{eGFP/eGFP}$ knock-in but not C57BL/6J ($S1pr1^{WT/WT}$) mice (Fig. 1B). This confirmed the specificity of the antibodies.

Therefore, we used the Duolink in situ PLA assay to study the molecular interaction between SR-BI and SIPRI-eGFP. This technique generates a red fluorescent signal only when SR-BI and SIPRI-eGFP are in close (<40 nm) proximity to each other. Peritoneal macrophages isolated from $S1pr1^{eGFP/eGFP}$ knock-in and WT

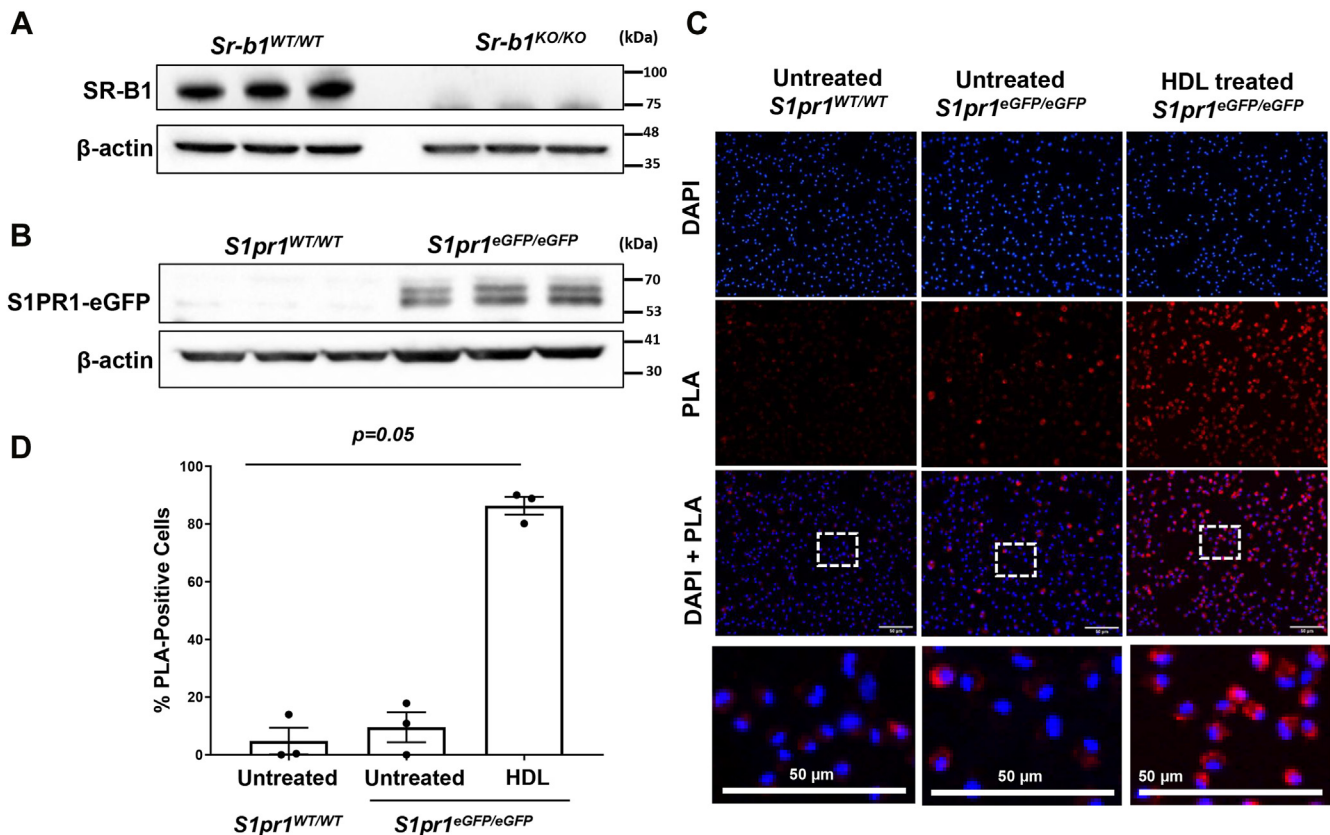


Fig. 1. SR-BI interacts with SIPRI-eGFP in murine macrophages in an HDL-dependent manner. Thioglycolate-elicited peritoneal macrophages were prepared from (A) $Sr-b1^{WT/WT}$ (C57BL/6J) and $Sr-b1^{KO/KO}$ mice and (B–D) $S1pr1^{WT/WT}$ (C57BL/6J) and $S1pr1^{eGFP/eGFP}$ mice and cultured. A, B: Cells were lysed and protein extracts were prepared and analyzed by immunoblotting for SR-BI, the GFP tag on SIPRI-GFP, and β-actin. C: Macrophages were either untreated or treated in culture with 100 μg (protein)/ml HDL as indicated. Control cells were treated with an equivalent volume of vehicle. After 30 min, cells were fixed, and Duolink proximity ligation assay (PLA) was performed (red fluorescence) as described in the ‘Materials and methods’ section. Nuclei were stained using DAPI (blue). C: Representative images (scale bars represent 50 μm; bottom row shows zoomed-in view of the boxed areas of the DAPI + PLA merged images) and (D) quantification of PLA signal performed by counting the proportion of cells exhibiting PLA signal across three fields of view for each sample well. Data are means ± SEM of $n = 3$ samples. Each data point represents cells isolated from a different mouse. Data were analyzed using the Kruskal-Wallis test and the P -value is indicated. eGFP, enhanced green fluorescent protein; PLA, proximity ligation assay; SIPR, sphingosine-1-phosphate receptor; SR-BI, scavenger receptor class B, type I.

control mice (lacking the eGFP tag on SIPRI) were treated for 30 min in the presence or absence of HDL and subjected to the Duolink in situ PLA assay. In the absence of HDL, there was little detectable PLA signal in WT macrophages lacking the eGFP tag on SIPRI, whereas a low level of signal was detected in *S1pr1^{eGFP/eGFP}* knock-in macrophages. In contrast, *S1pr1^{eGFP/eGFP}* knock-in macrophages in the presence of HDL exhibited a robust PLA signal (Fig. 1C, D), indicating that HDL stimulates the physical interaction between SR-BI and SIPRI receptors expressed endogenously in mouse primary macrophages in culture.

HDL-associated SIP promotes the interaction between SR-BI and SIPRI

To test if SIP was required for the interaction between SIPRI and SR-BI, HDL was pre-treated for 1 h with SIPL prior to incubation with cells. In parallel,

control HDL was mock treated in the absence of SIPL prior to adding it to the cells. In a separate experiment, we confirmed that SIPL treatment of HDL did not affect its elution profile on gel-filtration chromatography, as measured by absorbance at 280 nm, for protein, total cholesterol assays of fractions, or immunoblotting for apoA1 (the main structural protein on HDL) or apoM (the carrier of SIP on HDL) (supplemental Fig. 1A–D). The stimulation of the molecular interaction between SR-BI and SIPRI-eGFP by HDL was significantly reduced when HDL was pre-treated with SIPL compared to control HDL (Fig. 2A). In a separate experiment, we examined if SIP alone could promote the interaction between these two receptors. After incubating the *S1pr1^{eGFP/eGFP}* macrophages with SIP for 30 min, a slight increase in the average PLA signal was apparent, but this did not reach statistical significance. In parallel, *S1pr1^{eGFP/eGFP}*

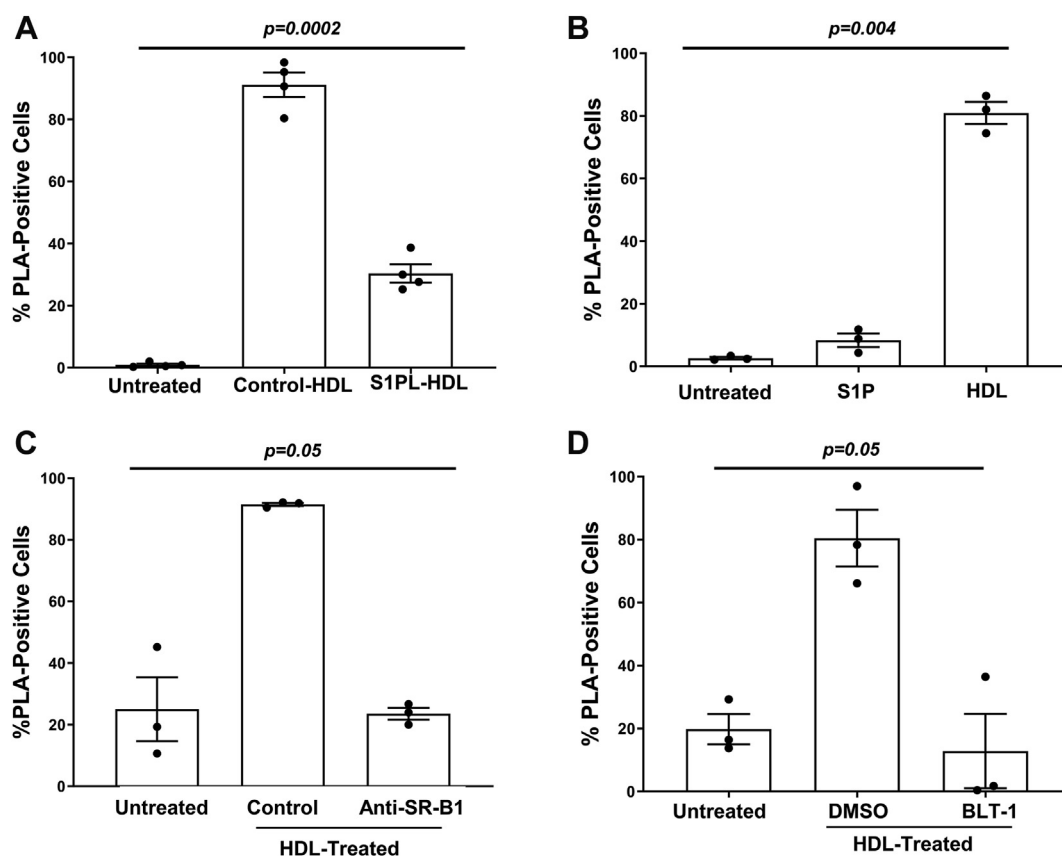


Fig. 2. The HDL-stimulated interaction between SR-BI and SIPRI is inhibited by SIPL treatment and by inhibition of SR-BI. Thioglycolate-elicited peritoneal macrophages were prepared from *S1pr1^{eGFP/eGFP}* mice. A: Cells were incubated for 30 min with HDL that had been pre-treated for 60 min at 37°C with SIPL or with control HDL pre-treated in parallel without SIPL. B: Cells were incubated for 30 min with either SIP (10 nM) or HDL (100 µg protein/ml). C: Cells were pre-treated in culture for 45 min with either an SR-BI blocking rabbit antiserum or a control, non-immune rabbit antiserum (each at 1.5 µg/ml), as indicated, before the addition of HDL (100 µg protein/ml). D: Cells were pre-treated for 45 min with either BLT-1 (150 nM added in DMSO) or an equivalent amount of DMSO vehicle control. HDL was then added. For each experiment, control cells were also incubated in media in the absence of added HDL (Untreated). After addition of HDL or vehicle, cells were incubated at 37°C for 30 min prior to being washed, fixed, and subjected to the Duolink PLA assay and staining for DAPI. Quantification of PLA signal was performed by counting the proportion of cells exhibiting PLA signal across five fields of view for each sample well. Data are means ± SEM of n = 4 (A) or n = 3 samples (B–D), where each replicate represents cells isolated from a different mouse. Data were analyzed using the Kruskal-Wallis test. P-values are indicated. eGFP, enhanced green fluorescent protein; PLA, proximity ligation assay; SIP, sphingosine-1-phosphate; SIPR, sphingosine-1-phosphate receptor; SIPL, SIPL-lyase; SR-BI, scavenger receptor class B, type I.

macrophages incubated for 30 min with HDL showed a robust increase in the PLA signal (Fig. 2B). These results demonstrate that SIP is necessary for HDL to fully stimulate the interaction between SR-BI and SIPRI-eGFP in macrophages and that SIP alone (in the absence of HDL) is not sufficient to stimulate the interaction.

Inhibition of SR-BI attenuates the HDL-stimulated interaction between SR-BI and SIPRI

To test the involvement of the extracellular domain of SR-BI in the HDL-stimulated interaction between SR-BI and SIPRI-eGFP, peritoneal macrophages from *Sipr1^{eGFP/eGFP}* mice were pre-treated for 45 min with an antibody (rabbit anti-mSR-BI KKB-1 antibody), against the extracellular domain of SR-BI that was previously reported to block HDL binding (52). As a control, cells were treated in parallel with a non-immune anti-rabbit IgG antibody. HDL (100 µg protein/ml) was added and SR-BI/SIPRI-eGFP complex formation was measured using the Duolink PLA assay. Pre-incubation with the anti-SR-BI blocking antibody significantly reduced the PLA signal compared to cells pre-incubated with the control IgG antibody (Fig. 2C), demonstrating the involvement of SR-BI's extracellular domain in the HDL-stimulated interaction with SIPRI. It is not clear if this reflected immunological blockade of SR-BI's ability to bind HDL (thereby preventing HDL-stimulation) or steric hindrance of the interaction between SR-BI and SIPRI. We therefore explored the effect of BLT-1, a small molecule inhibitor of SR-BI's ability to transfer lipids between the bound HDL and cells. BLT-1 has been reported to covalently modify a cysteine side chain protruding into the hydrophobic channel of SR-BI resulting in the inhibition of SR-BI-mediated lipid transport but not HDL binding (22, 25, 53). Macrophages from *Sipr1^{eGFP/eGFP}* mice were pre-treated with 150 nM BLT-1, before the addition of HDL (100 µg protein/ml). Control cells were incubated with DMSO as a vehicle. BLT-1 treatment of cells prevented HDL from stimulating the association of SR-BI with SIPRI-eGFP (Fig. 2D), suggesting that SR-BI-mediated lipid transfer activity is necessary to trigger the interaction between these two receptors in macrophages.

SEW2871, an SIPRI-selective agonist, promotes and Ex26, an SIPRI-selective antagonist, inhibits the interaction between SR-BI and SIPRI

We examined the effect of treating primary mouse macrophages with SEW2871, a selective agonist of SIPRI, on the physical interaction between SR-BI and SIPRI. Treatment of macrophages with 1 µM of SEW2871 for 30 min increased the PLA signal between SR-BI and SIPRI-eGFP to a similar extent as that triggered by HDL (Fig. 3A). To determine if inhibition of SR-BI's lipid transfer activity affected SEW2871-mediated SR-BI/SIPRI-eGFP interaction, macrophages were pre-treated with or without BLT-1 or with

the SR-BI-blocking antibody for 45 min. Cells were then incubated with SEW2871 for 30 min. Interestingly, the PLA signal induced by SEW2871 was significantly reduced by treatment with either BLT-1 or the anti-SR-BI-blocking antibody (Fig. 3A). These findings suggest that SR-BI activity is required for the SEW2871-stimulated interaction between SR-BI and SIPRI-eGFP, even in the absence of HDL.

To examine the effect of inhibiting SIPRI activity on the HDL-stimulated interaction between SR-BI and SIPRI, we used a selective antagonist for SIPRI called Ex26 (54). Primary mouse peritoneal macrophages isolated from *Sipr1^{eGFP/eGFP}* mice were first pre-treated for 1 h with 10 µM Ex26 or DMSO as a control, followed by incubation with HDL (100 µg protein/ml) for 30 min. Treatment of cells with Ex26 significantly reduced (86%) the HDL-stimulated interaction between SR-BI and SIPRI-eGFP. This result confirms that the activity of SIPRI is critical for its molecular interaction with SR-BI in cultured macrophages (Fig. 3B). To visualize the distribution of HDL-stimulated SR-BI/SIPRI complexes within macrophages and the effects of Ex26-mediated antagonism of SIPRI, macrophages from *Sipr1^{eGFP/eGFP}* mice were either untreated or treated with DMSO solvent control or HDL in the absence or presence of Ex26, fixed, permeabilized, and subjected to the Duolink PLA staining along with staining for caveolin-1 and imaged by confocal microscopy (Fig. 3C). HDL treatment dramatically increased punctate PLA signal throughout the cells in regions that did not coincide with staining for caveolin-1. Ex26 treatment reduced the numbers without noticeably affecting the distribution of PLA-positive punctae. Separate samples were stained with green fluorescently labeled WGA (to label the cell surface) prior to permeabilization and PLA staining, demonstrating similar effects of HDL Ex26 (supplemental Fig. S2).

Effects of inhibition of SR-BI or SIPRI on HDL-mediated cholesterol efflux and protection of macrophages against apoptosis

We next wanted to test if these treatments that interfered with HDL-stimulated SR-BI and SIPRI complex formation impacted HDL-mediated cholesterol efflux from macrophages. HDL-mediated cholesterol efflux was measured using a cholesterol efflux assay kit in which cells were pre-loaded with a fluorescently labeled analog of cholesterol, and efflux was initiated by the addition of HDL or SIPL-treated HDL for 3 h. Baseline efflux in the absence of added HDL as a cholesterol acceptor or in the presence of DMSO as a solvent control was also measured. This demonstrated that addition of control HDL triggered a substantial 3-fold increase in the efflux of cholesterol after 3 h as compared to basal efflux without a cholesterol acceptor (Fig. 4). In contrast, SIPL treatment of HDL prior to its addition to cells reduced cholesterol efflux by approximately 40% compared to untreated HDL. Treatment of cells with

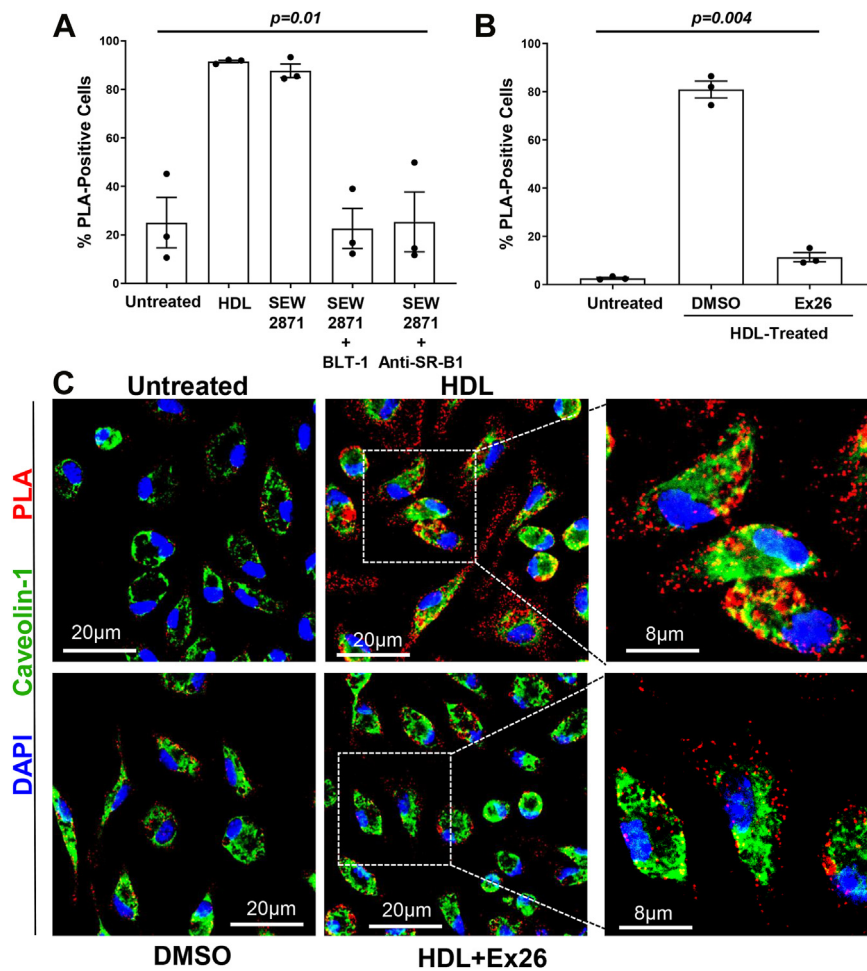


Fig. 3. The SIPR1 selective agonist, SEW2871, stimulates and the selective antagonist Ex26 inhibits the interaction between SR-BI and SIPR1. Thioglycolate-elicited peritoneal macrophages from *Sipr1^{eGFP/eGFP}* mice were (A) pre-treated with either the anti-SR-BI antiserum (1.5 µg/ml) or the SR-BI inhibitor BLT-1 (150 nM) for 45 min or with control non-immune rabbit serum and DMSO vehicle (where not indicated). After the pre-treatment period, HDL (100 µg protein/ml) or the SIPR1 selective agonist, SEW2871 (1 µM) or no stimulus (untreated) was added for an additional 30 min before cells were fixed. B: Cells were treated with either Ex26 (10 µM, added as a 1,000× stock in DMSO) or DMSO vehicle control for 60 min, at which point HDL (100 µg protein/ml) or vehicle was added and cells were incubated for a further 30 min. After the 30 min incubation with HDL, cells were washed, fixed, and subjected to Duolink PLA and DAPI staining, imaging, and analysis as in the legend to Figs. 1 and 2. Each symbol represents cells isolated from a different mouse. Data were analyzed using Kruskal-Wallis test; *P*-values are indicated above each graph. C: Thioglycolate-elicited peritoneal macrophages from *Sipr1^{eGFP/eGFP}* mice were incubated for 60 min with 10 µM Ex26 or DMSO vehicle control followed by treatment without or with HDL (100 µg protein/ml) for 30 min as indicated. Cells were then washed and fixed, and PLA staining (red) was carried out followed by staining for caveolin-1 using a mouse anti-caveolin-1 antibody and Alexa488-conjugated anti-mouse secondary antibody (green) and DAPI staining (blue). Panels on the right show zoomed-in views of the boxed areas of the merged images of HDL-treated control and Ex26-treated cells. eGFP, enhanced green fluorescent protein; PLA, proximity ligation assay; SIPR, sphingosine-1-phosphate receptor; SR-BI, scavenger receptor class B, type I.

either the SIPR1 antagonist, Ex26, or BLT-1, the inhibitor of SR-BI-mediated lipid transport, resulted in similar levels of inhibition of cholesterol efflux to HDL. This suggests that SIPL treatment and antagonism of SIPR1 are each able to reduce HDL-mediated cholesterol efflux to the same extent as inhibition of SR-BI but do not impact SR-BI-independent HDL-mediated cholesterol efflux pathways.

We have previously demonstrated that HDL can protect macrophages from apoptosis induced by different agents including tunicamycin and thapsigargin, both of which induce ER stress and UV irradiation and that this can be inhibited by knockout of

SIPR1 expression (5, 30, 34). Consistent with our previously reported findings, tunicamycin treatment of macrophages cultured in serum depleted of lipoproteins triggered increased apoptosis, measured by TUNEL staining for fragmented DNA (Fig. 5A, B). Cotreatment with HDL prevented the tunicamycin-stimulated apoptosis. However, the SR-BI inhibitor, BLT-1, largely prevented the HDL-mediated protection of macrophages against tunicamycin-induced apoptosis demonstrating that this property of HDL was dependent on SR-BI (Fig. 5A, B). SIPL pretreatment of HDL similarly inhibited HDL-mediated protection against tunicamycin-induced macrophage apoptosis (Fig. 5C).

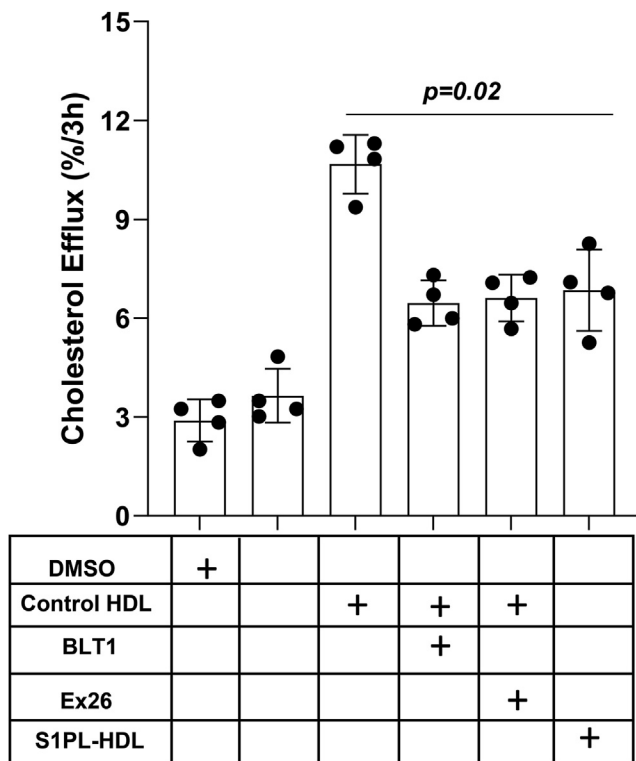


Fig. 4. The SR-BI inhibitor, BLT-1, the SIPRI antagonist Ex26, and SIPL treatment of HDL all reduce HDL-mediated cholesterol efflux from macrophages. Thioglycolate-elicited peritoneal macrophages were collected from wild type C57BL/6J mice, cultured in DMEM containing 10% FBS, 2 mM L-glutamine, 50 µg/ml penicillin, and 50 U/ml streptomycin, for 16 h prior to changing the medium to phenol red-free DMEM containing 3% newborn calf lipoprotein-deficient serum, 2 mM L-glutamine, 50 µg/ml penicillin, and 50 U/ml streptomycin, for an additional 16 h as described above. Cholesterol efflux was measured using the cell-based fluorescent Cholesterol Efflux Assay kit. After loading cells with the fluorescent tracer for 1 h, cells were washed and efflux was initiated by addition of the efflux acceptor medium. Efflux was monitored using either no acceptor or control- or SIPL-treated HDL (each at 100 µg protein/ml) as cholesterol acceptors. Some cells were also treated with Ex26 (10 µM) or BLT-1 (150 nM) during efflux. Cholesterol efflux was measured as the amount of cholesterol tracer appearing in the medium at the end of 3 h, as a % of the total cholesterol tracer (cells + medium). Each symbol represents cells isolated from a different mouse (n = 4); bars represent means and error bars represent standard errors. Data was analyzed by the Kruskal-Wallis test; P value is indicated. SIPL, SIPL-lyase; SIPR, sphingosine-1-phosphate receptor; SR-BI, scavenger receptor class B, type I.

These findings demonstrated that treatments which prevented HDL-stimulated SR-BI and SIPRI complex formation in macrophages also inhibited SR-BI-dependent, HDL-mediated cholesterol efflux and protection of macrophages against tunicamycin-induced apoptosis.

SR-BI and SIPRI form complexes in macrophages within atherosclerotic plaques

To examine whether SR-BI and SIPRI form complexes in cells in vivo, spleens and adrenal glands were

collected from *Sipr1^{eGFP/eGFP}* and control *Sipr1^{WT/WT}* mice, and PLA staining for SR-BI and SIPRI-eGFP interactions was carried out on cryosections of these tissues. PLA signal was detected in the sections of spleens (a tissue rich in immune cells, including macrophages) and in adrenal glands (a tissue known to express high levels of both SR-BI and SIPRI) from *Sipr1^{eGFP/eGFP}* but not *Sipr1^{WT/WT}* mice, expressing normal untagged SIPRI (supplemental Fig. S3). To test if SR-BI and SIPRI form complexes in cells within atherosclerotic plaques, we generated *Sipr1^{eGFP/eGFP}/ApoE^{KO/KO}* mice and fed them a high fat, high cholesterol, atherogenic diet for 8 weeks to promote atherosclerosis development in their aortic sinuses. As a negative control, we included atherogenic diet-fed *ApoE^{KO/KO}* mice (referred to as *Sipr1^{WT/WT}/ApoE^{KO/KO}* to emphasize that the SIPRI protein did not contain the eGFP tag). We also treated a subset of the atherogenic diet-fed *Sipr1^{eGFP/eGFP}/ApoE^{KO/KO}* mice with the Ex26 to antagonize SIPRI 12 h before harvest (control mice were treated in parallel with DMSO vehicle). Histological sections of atherosclerotic plaques in the aortic sinus from these mice were stained with oil red O (for neutral lipids) and hematoxylin for nuclei, to visualize atherosclerotic plaques (Fig. 6A). Adjacent cryosections were subjected to Duolink PLA staining using primary antibodies against the C-terminal cytoplasmic region of SR-BI and the cytoplasmic GFP tag of SIPRI-eGFP (Fig. 6B). We detected abundant PLA signal in atherosclerotic plaques from *Sipr1^{eGFP/eGFP}/ApoE^{KO/KO}* mice as compared to those from *Sipr1^{WT/WT}/ApoE^{KO/KO}* mice (Fig. 6B, C). Furthermore, the treatment of *Sipr1^{eGFP/eGFP}/ApoE^{KO/KO}* mice with Ex26 significantly reduced PLA signal to background levels seen in the plaques from *Sipr1^{WT/WT}/ApoE^{KO/KO}* mice (Fig. 6B, C). Co-staining of sections through atherosclerotic plaques for the macrophage marker Mac3 together with PLA staining for SR-BI and SIPRI-GFP complexes, together with confocal imaging at high magnification (Fig. 6D), revealed that the PLA signal was largely associated with Mac3-expressing cells within atherosclerotic plaques. These results suggest that SR-BI and SIPRI-GFP physically interacted in macrophages within the atherosclerotic plaque of experimental mice in a manner that requires activity of SIPRI, consistent with the interactions between SR-BI and SIPRI in cultured macrophages.

DISCUSSION

It has previously been reported that SR-BI and SIPRI form ligand-dependent complexes when they are overexpressed in transfected HEK293 cells and that HDL mediated calcium signaling in a manner dependent on both of these receptors (49). However, whether SR-BI/SIPRI complex formation also occurs at much lower levels of endogenous expression of the two receptors in primary cells in culture or in vivo was not tested. We have previously reported that SR-BI and SIPRI are both required for HDL signaling in primary

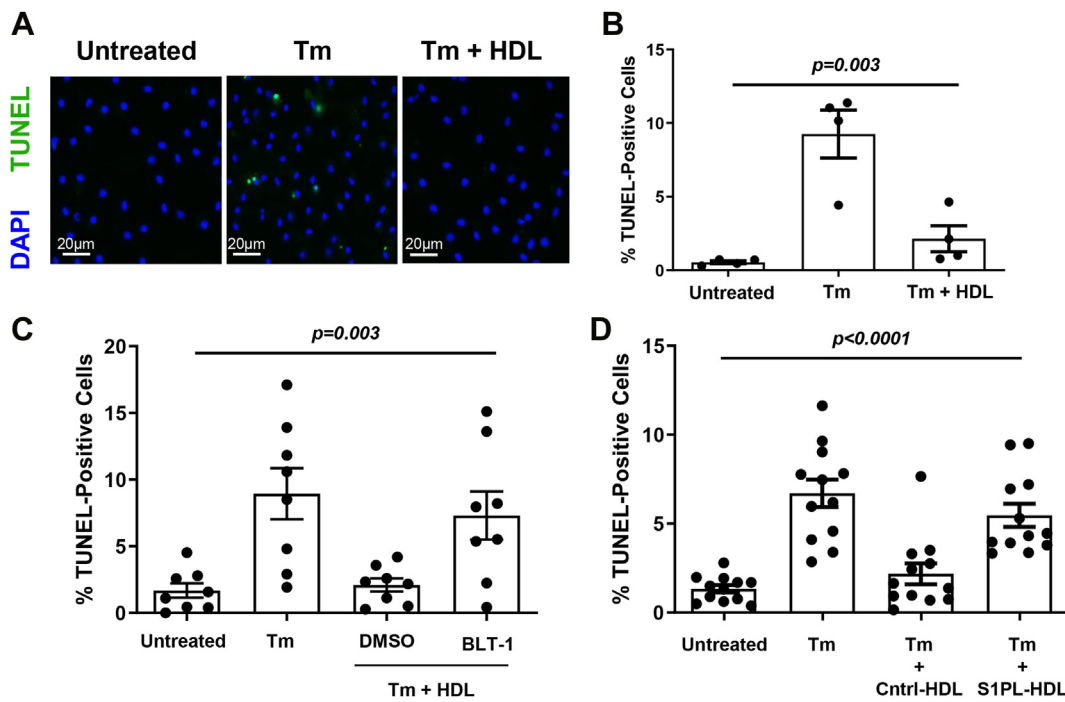


Fig. 5. HDL-mediated protection of macrophages from tunicamycin-induced apoptosis is inhibited by the SR-B1 inhibitor BLT-1 and by SIPL-treatment of HDL. Thioglycolate-elicited peritoneal macrophages from wild type C57BL/6J mice were cultured in 8-well chamber slides in DMEM containing 3% newborn calf lipoprotein-deficient serum for 16 h prior to the addition of (A, B) tunicamycin (10 $\mu\text{g}/\text{ml}$) without or with HDL (50 μg protein/ml), (C) tunicamycin (10 $\mu\text{g}/\text{ml}$), HDL (50 μg protein/ml), and BLT-1 (150 nM) or combinations of those as indicated; or (D) tunicamycin (10 $\mu\text{g}/\text{ml}$) and either SIPL-treated or control-treated HDL (50 μg protein/ml) as indicated. After 24 h, cells were fixed and apoptosis was detected by TUNEL staining for fragmented DNA, followed by counter-staining with DAPI for nuclear DNA. A: Representative images of TUNEL (green fluorescence) and DAPI (blue fluorescence) stained nuclei. B–D: Quantification of the degree of apoptosis (% TUNEL-positive nuclei). Each data point in (B) represents cells isolated from a different mouse ($n = 4$). Data points in (C) and (D) represent independent wells of cells isolated from 2 to 4 mice, plated in triplicate. Data were analyzed by the Kruskal-Wallis test; P values are indicated above each graph. SIPL, SIPL-lyase; TUNEL, Terminal deoxynucleotidyl transferase-mediated dUTP Nick End Labeling; SR-B1, scavenger receptor class B, type I.

murine macrophages leading to Akt phosphorylation, and others have shown that SIPR1 is required for HDL-mediated activation of signal transducer and activator of transcription 3 in macrophages and that these signaling pathways lead to chemotaxis and/or protection against cell death (5, 6, 28, 30, 35). Therefore, we set out to test if SR-B1 and SIPR1 formed complexes in primary murine macrophages in culture and in atherosclerotic plaques, largely comprised of macrophage-like foam cells. To do this, we made use of the Duolink PLA. This uses antibodies tagged with oligonucleotides: When the antibodies target two members of a protein complex and bring the oligonucleotide tags within 40 nm of each other, they can be ligated and amplified, incorporating fluorescent probes which are visualized by fluorescence microscopy. In order to do this, we screened a number of commercially available antibodies reported to target SIPR1, making use of macrophages from mice with a myeloid-specific *Sipr1* gene knockout that we have previously generated (30). Unfortunately, all the anti-SIPR1 antibodies that we tested exhibited substantial immunofluorescence signal in the macrophages lacking *Sipr1* gene expression (not shown). To overcome the

difficulty of finding an antibody suitably specific for SIPR1, we made use of a line of mice in which the complementary DNA for eGFP was knocked in-frame into the *Sipr1* gene such that the modified gene encoded a fusion protein in which the full-length SIPR1 protein contained eGFP fused to its cytoplasmic carboxy-terminus (51). Importantly, these mice express normal endogenous levels of the SIPR1-eGFP fusion protein, which exhibits normal function (51). Using a commercially available antibody against eGFP and an antibody against the cytoplasmic carboxy-terminus of SR-B1, in conjunction with the Duolink PLA, we report that, at endogenous expression levels in primary macrophages in culture and in cells in atherosclerotic plaques, SR-B1 and SIPR1 form complexes in response to HDL or to an SIPR1 agonist, SEW2871. Furthermore, the stimulation of formation of these complexes is blocked by an antibody that binds to the extracellular domain of SR-B1, an inhibitor (BLT-1) which blocks SR-B1's lipid transport activity, and an antagonist of SIPR1 signaling (Ex26).

The majority of SIP in plasma is carried by HDL (55), and HDL-bound SIP has been reported to act as a biased ligand for SIPR1 in endothelial cells (32).

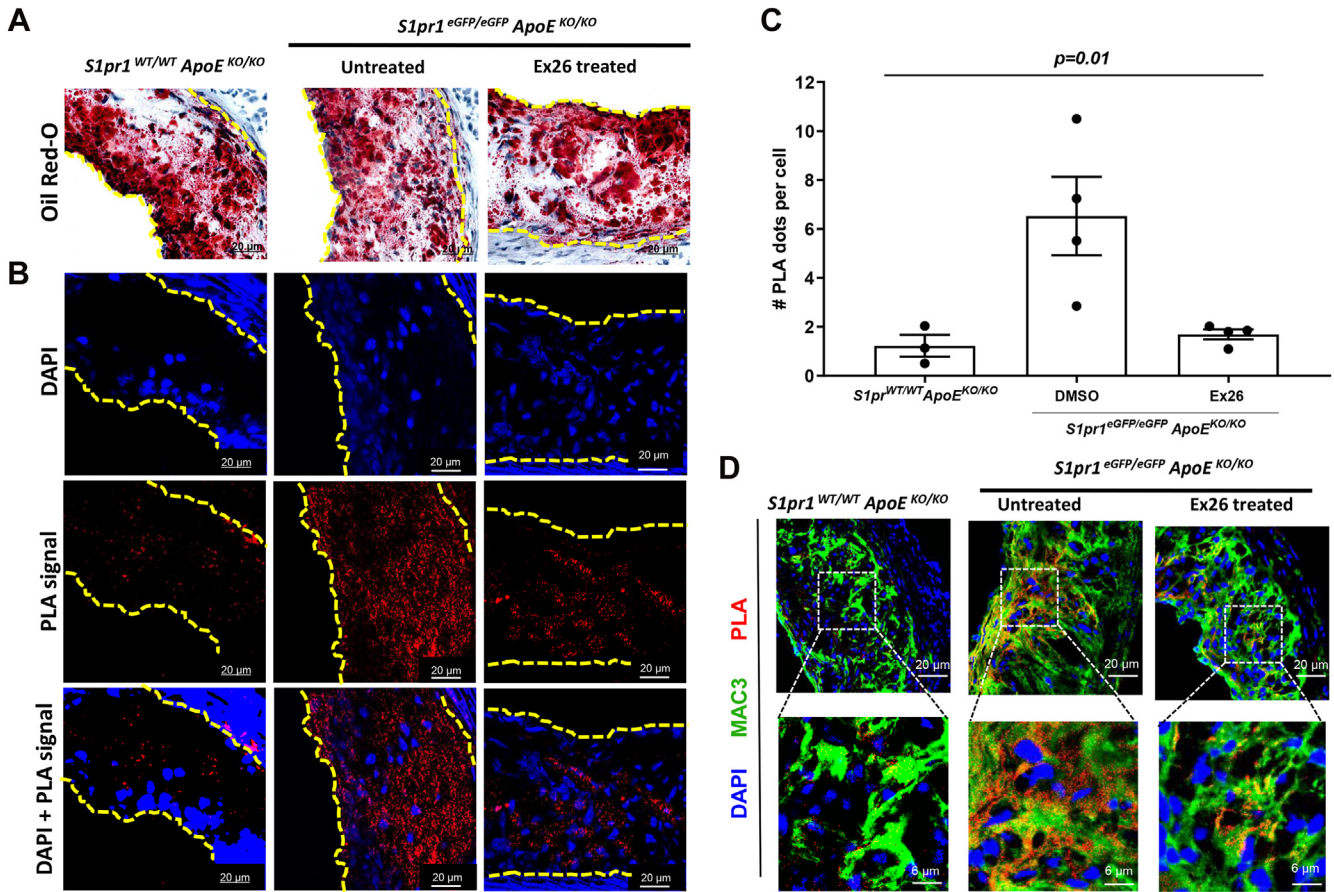


Fig. 6. SR-B1 and SIPRI interact in atherosclerotic plaques of high-fat diet-fed *ApoE^{KO/KO}* mice. Control *ApoE^{KO/KO}* mice in which SIPRI was not GFP tagged (*S1pr1^{WT/WT}/ApoE^{KO/KO}* mice), and *S1pr1^{eGFP/eGFP} ApoE^{KO/KO}* mice were fed a high fat, high cholesterol diet for 8 weeks, beginning at 15 weeks of age. *S1pr1^{eGFP/eGFP} ApoE^{KO/KO}* mice were then treated with Ex26 (30 mg/kg in DMSO) or DMSO vehicle and mice were euthanized, and tissues were harvested 12 h later. Adjacent cross-sections in the aortic sinus were collected and stained with oil red O (lipid) and hematoxylin (nuclei) to detect lipid-rich atherosclerotic plaques or were fixed, permeabilized, and subjected to Duolink PLA staining using antibodies against SR-B1 and GFP as described in the ‘Materials and methods’ section. PLA-stained sections were counterstained with DAPI for nuclear DNA. **A:** Representative images of oil red O and hematoxylin-stained atherosclerotic plaques in the aortic sinuses. **B:** Images of adjacent PLA-stained sections of plaques showing DAPI, PLA signal, and merged DAPI and PLA signals. Scale bars (A, B) represent 20 μ m. **C:** Quantification of PLA signal in the atherosclerotic plaques of *S1pr1^{WT/WT}/ApoE^{KO/KO}* and DMSO vehicle or Ex26-treated *S1pr1^{eGFP/eGFP} ApoE^{KO/KO}* mice was performed by counting the average of PLA signal puncta within atherosclerotic plaques across three fields of view per plaque of three sections for each mouse and dividing by the number of DAPI-stained nuclei. Each data point represents data from a different mouse. Data were analyzed using the Kruskal-Wallis test; *P* value is indicated above the graph. **D:** Confocal images of PLA (red) and anti-Mac3 immunofluorescence (green) and DAPI (blue) co-stained images of atherosclerotic plaques from control *S1pr1^{WT/WT}/ApoE^{KO/KO}* and DMSO vehicle or Ex26-treated *S1pr1^{eGFP/eGFP} ApoE^{KO/KO}* mice. Images in the bottom row correspond to zoomed-in views of the boxed areas. eGFP, enhanced green fluorescent protein; PLA, proximity ligation assay; SIPR, sphingosine-1-phosphate receptor; SR-B1, scavenger receptor class B, type I.

Furthermore, HDL signaling in endothelial cells requires SR-B1 and SIPRI (32, 37, 56, 57). We reported that HDL stimulation of Akt phosphorylation, macrophage migration, and protection of macrophages against apoptosis are lost when SIPRI is knocked out or functionally antagonized, suggesting that HDL stimulation of these responses by macrophages are dependent on SIPRI signaling (28, 30). Likewise, we found that HDL stimulation of SR-B1/SIPRI-GFP complex formation in macrophages in culture is prevented by an antagonist of SIPRI, or by SIPL, an enzyme that irreversibly converts SIP into ethanolamine and a fatty aldehyde, neither of which are able to elicit SIPRI signaling. This indicates that HDL stimulation of SR-B1 and SIPRI complex formation is dependent on SIP. In contrast,

SIP added in the absence of a lipoprotein carrier did not stimulate SR-B1/SIPRI complex formation. These results in macrophages are consistent with what was previously reported in HEK293 cells overexpressing both recombinant SIPRI and SR-B1, where it was shown that SIP is a necessary component of HDL, but this bioactive sphingolipid is not sufficient for promoting the SR-B1/SIPRI interaction on its own (49). These findings are consistent with the idea proposed by others that HDL-associated SIP acts as a biased ligand for SIPRI, eliciting responses distinct from those elicited by SIP that is not delivered by HDL (32, 58). Unlike SIP, however, the synthetic SIPRI-specific agonist, SEW2871, was able to stimulate SR-B1/SIPRI complex formation in macrophages in the absence of lipoprotein carriers.

However, SEW2871-mediated SR-BI/SIPRI complex formation was also inhibited by BLT-1. This suggests that SR-BI may play a role in the delivery of SEW2871 to SIPRI, thereby facilitating its activation.


When HDL pre-treated with SIPL was used or when cells were incubated with the SIPRI antagonist, Ex26, HDL-mediated cholesterol efflux was reduced to similar levels as that observed when cells were treated with the SR-BI transport inhibitor, BLT-1. This suggests that SIP contributes to HDL-mediated cholesterol efflux from macrophages, likely as a result of SIPRI signaling and through SR-BI-mediated cholesterol transport (since the SIPRI antagonist and the SR-BI transport inhibitor both reduced HDL-mediated efflux to the same extent as SIPL treatment). SIP has previously been implicated in the regulation of ABCA1-mediated cholesterol efflux through the SIPR3 receptor (59, 60). Our findings demonstrate that SIP similarly regulates HDL-mediated cholesterol efflux through SR-BI and implicate SR-BI/SIPRI complex formation in this process. Similarly, HDL-mediated protection against tunicamycin-induced apoptosis was reduced either when HDL was pretreated with SIPL or when cells were incubated with the SR-BI inhibitor. This suggests that treatments which prevented HDL-mediated SR-BI and SIPRI complex formation also impacted HDL-dependent protection against apoptosis, suggesting a role for SR-BI and SIPRI complex formation in this process as well.

In addition to demonstrating that SR-BI and SIPRI form complexes in primary macrophages in culture, we demonstrated that SR-BI and SIPRI form complexes in cells within spleens and in adrenal glands (known to highly express SR-BI) of *Sipr1^{eGFP/eGFP}* mice as well as in macrophages within atherosclerotic plaques in *Sipr1^{eGFP/eGFP}/ApoE^{KO/KO}* mice fed a high fat diet. Macrophages and macrophage-like foam cells make up the majority of cells within atherosclerotic plaques (2). Furthermore, we demonstrated that treatment of high fat diet-fed *Sipr1^{eGFP/eGFP}/ApoE^{KO/KO}* mice with Ex26 disrupted SR-BI/SIPRI complexes in atherosclerotic plaque macrophages. Ex26 is a specific antagonist of SIPRI which also reportedly inhibits its internalization and degradation (61). These findings suggest that the activity of SIPRI is required for its interaction with SR-BI in macrophages both in culture and within murine atherosclerotic plaques. These findings, along with our demonstration that the disruption of SR-BI/SIPRI complex formation is associated with reductions in SR-BI-mediated HDL functions including cholesterol efflux and protection against apoptosis, suggest that SR-BI/SIPRI complex formation in macrophages may play an important role in these atheroprotective pathways in vivo. Our previous demonstration that SIPRI knockout in myeloid cells, which include macrophages, accelerates diet-induced atherosclerotic plaque development in LDLR-deficient mice is consistent with this (30).

The mechanisms and stoichiometry of SR-BI and SIPRI complex formation are unclear and require further investigation. Both SR-BI and SIPRI have been reported previously to be at least partially localized to cholesterol-rich lipid rafts or plasma membrane domains enriched in caveolin-1 (20, 62, 63). However, the SR-BI/SIPRI complexes identified by the PLA signal do not appear to colocalize with caveolin-1 in cultured macrophages, suggesting that they are not located in cholesterol-rich caveolae. SR-BI and SIPRI complexes are not confined to macrophages since we have also detected them in the sections of adrenal glands. Adrenocortical cells in the adrenal gland are known to express very high levels of SR-BI protein and also express SIPRI (20, 64). The role that SR-BI/SIPRI complexes play in adrenocortical cell functions such as HDL-cholesterol uptake or steroid hormone biosynthesis remains to be explored.

In conclusion, our study demonstrates that HDL can stimulate the molecular interaction between SIPRI and SR-BI proteins expressed at endogenous levels in murine macrophages in culture and within atherosclerotic plaques. Both SR-BI and SIPRI have been reported to be required for HDL signaling in macrophages and other cell types. The observation that these receptors form complexes in macrophages in culture and within experimental atherosclerotic plaques provides insights into the mechanisms by which they are both involved in HDL signaling in macrophages and suggests that this may impact atherosclerotic plaque development. We have previously demonstrated that HDL-mediated protection of macrophages against cell death involves SIPRI (30) and SR-BI (6), and we and others have reported that KO of either SR-BI in bone marrow-derived cells (48, 65) or SIPRI in myeloid cells (30), both of which include macrophages, results in increased cell death in atherosclerotic plaques and increased atherosclerosis development. Similarly, SIPRI inactivation in endothelial cells also increased atherosclerosis (32). Furthermore, some studies have reported that treatment of mice with SIPRI agonists reduced atherosclerosis while other studies reported no effects on atherosclerotic plaque size (61, 66–68). Further research is needed to understand the importance of SIPRI signaling and the role of SR-BI/SIPRI complex formation for HDL signaling in macrophages as well as other cell types (endothelial and smooth muscle cells) during atherosclerosis development and whether this represents an opportunity for therapeutic intervention.

Data availability

The data described in the manuscript are available in the [Supplementary materials](#) or from B. Trigatti, McMaster University (trigatt@mcmaster.ca) upon request. 



Supplemental data

This article contains [supplemental data](#).

Author contributions

C. B. and B. L. T. writing—original draft; C. B., G. E. G. K., N. T., K. M. C., L. G., and B. L. T. writing—review and editing; C. B., G. E. G. K., and B. L. T. data curation; C. B., G. E. G. K., N. T., K. M. C., L. G., and B. L. T. formal analysis; C. B., G. E. G. K., N. T., K. M. C., and L. G. investigation; C. B., G. E. G. K., N. T., K. M. C., and L. G. methodology; B. L. T. conceptualization; B. L. T. funding acquisition; B. L. T. project administration; B. L. T. resources; B. L. T. supervision.

Author ORCIDs

Leticia Gonzalez  <https://orcid.org/0000-0002-0589-6884>
Bernardo L. Trigatti  <https://orcid.org/0000-0002-4556-119X>

Funding and additional information

This work was supported by the Canadian Institutes of Health Research (grant number PJT – 178225) to B. L. T. The sponsor had no involvement in the study design, collection, analysis or interpretation of data, writing of the manuscript, or the decision to submit the article for publication.

Conflict of interest

The authors declare that they have no conflicts of interest with the contents of this article.

Abbreviations

DMSO, dimethyl sulfoxide; eGFP, enhanced green fluorescent protein; ORO, oil red O; ox-LDL, oxidized LDL; PFA, paraformaldehyde; PLA, proximity ligation assay; RT, room temperature; SIP, sphingosine-1-phosphate; SIPL, SIPL-lyase; SIPR, sphingosine-1-phosphate receptor; SR-BI, scavenger receptor class B, type I; TUNEL, Terminal deoxynucleotidyl transferase-mediated dUTP Nick End Labeling; WGA, wheat germ agglutinin.

Manuscript received August 7, 2023, and in revised form March 16, 2024, Published, JLR Papers in Press, April 5, 2024, <https://doi.org/10.1016/j.jlr.2024.100541>

REFERENCES

1. Tuttolomondo, A., Di Raimondo, D., Pecoraro, R., Arnao, V., Pinto, A., and Licata, G. (2012) Atherosclerosis as an inflammatory disease. *Curr. Pharm. Des.* **18**, 4266–4288
2. Moore, K. J., and Tabas, I. (2011) Macrophages in the pathogenesis of atherosclerosis. *Cell* **145**, 341–355
3. Bekkering, S., Quintin, J., Joosten, L. A., van der Meer, J. W., Netea, M. G., and Riksen, N. P. (2014) Oxidized low-density lipoprotein induces long-term proinflammatory cytokine production and foam cell formation via epigenetic reprogramming of monocytes. *Arterioscler. Thromb. Vasc. Biol.* **34**, 1731–1738
4. Karunakaran, D., Geoffrion, M., Wei, L., Gan, W., Richards, L., Shangari, P., et al. (2016) Targeting macrophage necroptosis for therapeutic and diagnostic interventions in atherosclerosis. *Sci. Adv.* **2**, e1600224
5. Yu, P., Qian, A. S., Chathely, K. M., and Trigatti, B. L. (2018) PDZK1 in leukocytes protects against cellular apoptosis and necrotic core development in atherosclerotic plaques in high fat diet fed ldl receptor deficient mice. *Atherosclerosis* **276**, 171–181
6. Kluck, G. E. G., Qian, A. S., Sakarya, E. H., Quach, H., Deng, Y. D., and Trigatti, B. L. (2023) Apolipoprotein AI protects against necrotic core development in atherosclerotic plaques: PDZK1-dependent high-density lipoprotein suppression of necroptosis in macrophages. *Arterioscler. Thromb. Vasc. Biol.* **43**, 45–63
7. Wintergerst, E. S., Jelk, J., Rahner, C., and Asmis, R. (2000) Apoptosis induced by oxidized low density lipoprotein in human monocyte-derived macrophages involves CD36 and activation of caspase-3. *Eur. J. Biochem.* **267**, 6050–6059
8. Thorp, E., Subramanian, M., and Tabas, I. (2011) The role of macrophages and dendritic cells in the clearance of apoptotic cells in advanced atherosclerosis. *Eur. J. Immunol.* **41**, 2515–2518
9. Kavurma, M. M., Rayner, K. J., and Karunakaran, D. (2017) The walking dead: macrophage inflammation and death in atherosclerosis. *Curr. Opin. Lipidol.* **28**, 91–98
10. Choudhury, R. P., Rong, J. X., Trogan, E., Elmalem, V. I., Dansky, H. M., Breslow, J. L., et al. (2004) High-density lipoproteins retard the progression of atherosclerosis and favorably remodel lesions without suppressing indices of inflammation or oxidation. *Arterioscler. Thromb. Vasc. Biol.* **24**, 1904–1909
11. Emerging Risk Factors Collaboration, Di Angelantonio, E., Sarwar, N., Perry, P., Kaptoge, S., Ray, K. K., et al. (2009) Major lipids, apolipoproteins, and risk of vascular disease. *JAMA* **302**, 1993–2000
12. Gordon, T., Castelli, W. P., Hjortland, M. C., Kannel, W. B., and Dawber, T. R. (1977) High density lipoprotein as a protective factor against coronary heart disease: the Framingham study. *Am. J. Med.* **62**, 707–714
13. Shaw, J. A., Bobik, A., Murphy, A., Kanellakis, P., Blomberg, P., Mukhamedova, N., et al. (2008) Infusion of reconstituted high-density lipoprotein leads to acute changes in human atherosclerotic plaque. *Circ. Res.* **103**, 1084–1091
14. Feig, J. E., Hewing, B., Smith, J. D., Hazen, S. L., and Fisher, E. A. (2014) High-density lipoprotein and atherosclerosis regression: evidence from preclinical and clinical studies. *Circ. Res.* **114**, 205–213
15. Krieger, M. (1999) Charting the fate of the “Good cholesterol”: identification and characterization of the high-density lipoprotein receptor SR-BI. *Annu. Rev. Biochem.* **68**, 523–558
16. Lewis, G. F., and Rader, D. J. (2005) New insights into the regulation of HDL metabolism and reverse cholesterol transport. *Circ. Res.* **96**, 1221–1232
17. Trigatti, B. L., Rigotti, A., and Braun, A. (2000) Cellular and physiological roles of SR-BI, a lipoprotein receptor which mediates selective lipid uptake. *Biochim. Biophys. Acta* **1529**, 276–286
18. Acton, S., Rigotti, A., Landschulz, K. T., Xu, S., Hobbs, H. H., and Krieger, M. (1996) Identification of scavenger receptor SR-BI as a high density lipoprotein receptor. *Science* **271**, 518–520
19. Acton, S. L., Scherer, P. E., Lodish, H. F., and Krieger, M. (1994) Expression cloning of SR-BI, a CD36-related class B scavenger receptor. *J. Biol. Chem.* **269**, 21003–21009
20. Babbitt, J., Trigatti, B., Rigotti, A., Smart, E. J., Anderson, R. G., Xu, S., et al. (1997) Murine SR-BI, a high density lipoprotein receptor that mediates selective lipid uptake, is N-glycosylated and fatty acylated and colocalizes with plasma membrane caveolae. *J. Biol. Chem.* **272**, 13242–13249
21. Kartz, G. A., Holme, R. L., Nicholson, K., and Sahoo, D. (2014) SR-BI/CD36 chimeric receptors define extracellular subdomains of SR-BI critical for cholesterol transport. *Biochemistry* **53**, 6173–6182
22. Neculai, D., Schwake, M., Ravichandran, M., Zunke, F., Collins, R. F., Peters, J., et al. (2013) Structure of LIMP-2 provides functional insights with implications for SR-BI and CD36. *Nature* **504**, 172–176
23. Rodriguez, W. V., Thuahnai, S. T., Temel, R. E., Lund-Katz, S., Phillips, M. C., and Williams, D. L. (1999) Mechanism of scavenger receptor class B type I-mediated selective uptake of cholesteryl esters from high density lipoprotein to adrenal cells. *J. Biol. Chem.* **274**, 20344–20350
24. Thuahnai, S. T., Lund-Katz, S., Williams, D. L., and Phillips, M. C. (2001) Scavenger receptor class B, type I-mediated uptake of various lipids into cells. Influence of the nature of the donor particle interaction with the receptor. *J. Biol. Chem.* **276**, 43801–43808
25. Yu, M., Romer, K. A., Nieland, T. J., Xu, S., Saenz-Vash, V., Penman, M., et al. (2011) Exoplasmic cysteine Cys384 of the HDL receptor SR-BI is critical for its sensitivity to a small-molecule inhibitor and normal lipid transport activity. *Proc. Natl. Acad. Sci. U. S. A.* **108**, 12243–12248
26. Yu, M., Lau, T. Y., Carr, S. A., and Krieger, M. (2012) Contributions of a disulfide bond and a reduced cysteine side chain to the intrinsic activity of the high-density lipoprotein receptor SR-BI. *Biochemistry* **51**, 10044–10055

27. Mineo, C., and Shaul, P. W. (2013) Regulation of signal transduction by HDL. *J. Lipid Res.* **54**, 2315–2324
28. Al-Jarallah, A., Chen, X., Gonzalez, L., and Trigatti, B. L. (2014) High density lipoprotein stimulated migration of macrophages depends on the scavenger receptor class B, type I, PDZK1 and Akt1 and is blocked by sphingosine 1 phosphate receptor antagonists. *PLoS One.* **9**, e106487
29. Al-Jarallah, A., and Trigatti, B. L. (2010) A role for the scavenger receptor, class B type I in high density lipoprotein dependent activation of cellular signaling pathways. *Biochim. Biophys. Acta.* **1801**, 1239–1248
30. Gonzalez, L., Qian, A. S., Tahir, U., Yu, P., and Trigatti, B. L. (2017) Sphingosine-1-Phosphate receptor 1, expressed in myeloid cells, slows diet-induced atherosclerosis and protects against macrophage apoptosis in ldlr KO mice. *Int. J. Mol. Sci.* **18**, 2721
31. Poti, F., Simoni, M., and Nofer, J. R. (2014) Atheroprotective role of high-density lipoprotein (HDL)-associated sphingosine-1-phosphate (SIP). *Cardiovasc. Res.* **103**, 395–404
32. Galvani, S., Sanson, M., Blaho, V. A., Swendeman, S. L., Obinata, H., Conger, H., et al. (2015) HDL-bound sphingosine 1-phosphate acts as a biased agonist for the endothelial cell receptor SIP1 to limit vascular inflammation. *Sci. Signal.* **8**, ra79
33. Keul, P., Polzin, A., Kaiser, K., Graler, M., Dannenberg, L., Daum, G., et al. (2019) Potent anti-inflammatory properties of HDL in vascular smooth muscle cells mediated by HDL-SIP and their impairment in coronary artery disease due to lower HDL-SIP: a new aspect of HDL dysfunction and its therapy. *FASEB J.* **33**, 1482–1495
34. Yu, P., Qian, A. S., Chathely, K. M., and Trigatti, B. L. (2018) Data on leukocyte PDZK1 deficiency affecting macrophage apoptosis but not monocyte recruitment, cell proliferation, macrophage abundance or ER stress in atherosclerotic plaques of LDLR deficient mice. *Data Brief.* **19**, 1148–1161
35. Feuerborn, R., Becker, S., Poti, F., Nagel, P., Brodde, M., Schmidt, H., et al. (2017) High density lipoprotein (HDL)-associated sphingosine 1-phosphate (SIP) inhibits macrophage apoptosis by stimulating STAT3 activity and survivin expression. *Atherosclerosis.* **257**, 29–37
36. Nofer, J. R., Kehrel, B., Fobker, M., Levkau, B., Assmann, G., and von Eckardstein, A. (2002) HDL and arteriosclerosis: beyond reverse cholesterol transport. *Atherosclerosis.* **161**, 1–16
37. Kimura, T., Tomura, H., Mogi, C., Kuwabara, A., Damirin, A., Ishizuka, T., et al. (2006) Role of scavenger receptor class B type I and sphingosine 1-phosphate receptors in high density lipoprotein-induced inhibition of adhesion molecule expression in endothelial cells. *J. Biol. Chem.* **281**, 37457–37467
38. Assanasen, C., Mineo, C., Seetharam, D., Yuhanna, I. S., Marcel, Y. L., Connelly, M. A., et al. (2005) Cholesterol binding, efflux, and a PDZ-interacting domain of scavenger receptor-BI mediate HDL-initiated signaling. *J. Clin. Invest.* **115**, 969–977
39. Nofer, J. R. (2015) Signal transduction by HDL: agonists, receptors, and signaling cascades. *Handb. Exp. Pharmacol.* **224**, 229–256
40. Maceyka, M., Harikumar, K. B., Milstien, S., and Spiegel, S. (2012) Sphingosine-1-phosphate signaling and its role in disease. *Trends Cell Biol.* **22**, 50–60
41. Spiegel, S., and Milstien, S. (2003) Sphingosine-1-phosphate: an enigmatic signalling lipid. *Nat. Rev. Mol. Cell Biol.* **4**, 397–407
42. Zhang, B., Tomura, H., Kuwabara, A., Kimura, T., Miura, S., Noda, K., et al. (2005) Correlation of high density lipoprotein (HDL)-associated sphingosine 1-phosphate with serum levels of HDL-cholesterol and apolipoproteins. *Atherosclerosis.* **178**, 199–205
43. Sattler, K. J., Elbasan, S., Keul, P., Elter-Schulz, M., Bode, C., Graler, M. H., et al. (2010) Sphingosine 1-phosphate levels in plasma and HDL are altered in coronary artery disease. *Basic Res. Cardiol.* **105**, 821–832
44. Christoffersen, C., Obinata, H., Kumaraswamy, S. B., Galvani, S., Ahnstrom, J., Sevana, M., et al. (2011) Endothelium-protective sphingosine-1-phosphate provided by HDL-associated apolipoprotein M. *Proc. Natl. Acad. Sci. U. S. A.* **108**, 9613–9618
45. O'Sullivan, C., and Dev, K. K. (2013) The structure and function of the SIP1 receptor. *Trends Pharmacol. Sci.* **34**, 401–412
46. Chun, J., Hla, T., Lynch, K. R., Spiegel, S., and Moolenaar, W. H. (2010) International union of basic and clinical pharmacology. LXXVIII. Lysophospholipid receptor nomenclature. *Pharmacol. Rev.* **62**, 579–587
47. Blaho, V. A., and Hla, T. (2014) An update on the biology of sphingosine 1-phosphate receptors. *J. Lipid Res.* **55**, 1596–1608
48. Tao, H., Yancey, P. G., Babaev, V. R., Blakemore, J. L., Zhang, Y., Ding, L., et al. (2015) Macrophage SR-BI mediates efferocytosis via Src/PI3K/Rac1 signaling and reduces atherosclerotic lesion necrosis. *J. Lipid Res.* **56**, 1449–1460
49. Lee, M. H., Appleton, K. M., El-Shewy, H. M., Sorci-Thomas, M. G., Thomas, M. J., Lopes-Virella, M. F., et al. (2017) SIP in HDL promotes interaction between SR-BI and SIP1 and activates SIP1-mediated biological functions: calcium flux and SIP1 internalization. *J. Lipid Res.* **58**, 325–338
50. Rigotti, A., Trigatti, B. L., Penman, M., Rayburn, H., Herz, J., and Krieger, M. (1997) A targeted mutation in the murine gene encoding the high density lipoprotein (HDL) receptor scavenger receptor class B type I reveals its key role in HDL metabolism. *Proc. Natl. Acad. Sci. U. S. A.* **94**, 12610–12615
51. Cahalan, S. M., Gonzalez-Cabrera, P. J., Sarkisyan, G., Nguyen, N., Schaeffer, M. T., Huang, L., et al. (2011) Actions of a picomolar short-acting SIP(1) agonist in SIP(1)-eGFP knock-in mice. *Nat. Chem. Biol.* **7**, 254–256
52. Gu, X., Kozarsky, K., and Krieger, M. (2000) Scavenger receptor class B, type I-mediated [3H]cholesterol efflux to high and low density lipoproteins is dependent on lipoprotein binding to the receptor. *J. Biol. Chem.* **275**, 29993–30001
53. Nieland, T. J., Shaw, J. T., Jaipuri, F. A., Duffner, J. L., Koehler, A. N., Banakos, S., et al. (2008) Identification of the molecular target of small molecule inhibitors of HDL receptor SR-BI activity. *Biochemistry.* **47**, 460–472
54. Cahalan, S. M., Gonzalez-Cabrera, P. J., Nguyen, N., Guerrero, M., Cisar, E. A., Leaf, N. B., et al. (2013) Sphingosine 1-phosphate receptor 1 (SIP1) upregulation and amelioration of experimental autoimmune encephalomyelitis by an SIP1 antagonist. *Mol. Pharmacol.* **83**, 316–321
55. Murata, N., Sato, K., Kon, J., Tomura, H., Yanagita, M., Kuwabara, A., et al. (2000) Interaction of sphingosine 1-phosphate with plasma components, including lipoproteins, regulates the lipid receptor-mediated actions. *Biochem. J.* **352**, 809–815
56. Kimura, T., Tomura, H., Sato, K., Ito, M., Matsuoka, I., Im, D. S., et al. (2010) Mechanism and role of high density lipoprotein-induced activation of AMP-activated protein kinase in endothelial cells. *J. Biol. Chem.* **285**, 4387–4397
57. Kimura, T., Sato, K., Malchinkhuu, E., Tomura, H., Tamama, K., Kuwabara, A., et al. (2003) High-density lipoprotein stimulates endothelial cell migration and survival through sphingosine 1-phosphate and its receptors. *Arterioscler. Thromb. Vasc. Biol.* **23**, 1283–1288
58. Wilkerson, B. A., Grass, G. D., Wing, S. B., Argraves, W. S., and Argraves, K. M. (2012) Sphingosine 1-phosphate (SIP) carrier-dependent regulation of endothelial barrier: high density lipoprotein (HDL)-SIP prolongs endothelial barrier enhancement as compared with albumin-SIP via effects on levels, trafficking, and signaling of SIP1. *J. Biol. Chem.* **287**, 44645–44653
59. Vaidya, M., Jentsch, J. A., Peters, S., Keul, P., Weske, S., Graler, M. H., et al. (2019) Regulation of ABCA1-mediated cholesterol efflux by sphingosine-1-phosphate signaling in macrophages. *J. Lipid Res.* **60**, 506–515
60. Keul, P., Peters, S., von Wnuck Lipinski, K., Schroder, N. H., Nowak, M. K., Duse, D. A., et al. (2022) Sphingosine-1-phosphate (SIP) lyase inhibition aggravates atherosclerosis and induces plaque rupture in *ApoE*^{-/-} mice. *Int. J. Mol. Sci.* **23**, 9606
61. Poti, F., Gualtieri, F., Sacchi, S., Weißen-Plenz, G., Varga, G., Brodde, M., et al. (2013) KRP-203, sphingosine 1-phosphate receptor type I agonist, ameliorates atherosclerosis in LDLR^{-/-} mice. *Arterioscler. Thromb. Vasc. Biol.* **33**, 1505–1512
62. Singleton, P. A., Dudek, S. M., Ma, S. F., and Garcia, J. G. (2006) Transactivation of sphingosine-1-phosphate receptors is essential for vascular barrier regulation. Novel role for hyaluronan and CD44 receptor family. *J. Biol. Chem.* **281**, 34381–34393
63. Badawy, S. M. M., Okada, T., Kajimoto, T., Hirase, M., Matovelo, S. A., Nakamura, S., et al. (2018) Extracellular α -synuclein drives sphingosine-1-phosphate receptor subtype 1 out of lipid rafts, leading to impaired inhibitory G-protein signaling. *J. Biol. Chem.* **293**, 8208–8216
64. Werth, S., Müller-Fielitz, H., and Raasch, W. (2017) Obesity-stimulated aldosterone release is not related to an SIP-dependent mechanism. *J. Endocrinol.* **235**, 251–265

65. Covey, S. D., Krieger, M., Wang, W., Penman, M., and Trigatti, B. L. (2003) Scavenger receptor class B type I-mediated protection against atherosclerosis in LDL receptor-negative mice involves its expression in bone marrow-derived cells. *Arterioscler. Thromb. Vasc. Biol.* **23**, 1589–1594
66. Keul, P., Tölle, M., Lucke, S., von Wnuck Lipinski, K., Heusch, G., Schuchardt, M., *et al.* (2007) The sphingosine-1-phosphate analogue FTY720 reduces atherosclerosis in apolipoprotein E-deficient mice. *Arterioscler. Thromb. Vasc. Biol.* **27**, 607–613
67. Nofer, J.-R., Bot, M., Brodde, M., Taylor, P. J., Salm, P., Brinkmann, V., *et al.* (2007) FTY720, a synthetic sphingosine 1 phosphate analogue, inhibits development of atherosclerosis in low-density lipoprotein receptor-deficient mice. *Circulation.* **115**, 501–508
68. Potì, F., Costa, S., Bergonzini, V., Galletti, M., Pignatti, E., Weber, C., *et al.* (2012) Effect of sphingosine 1-phosphate (S1P) receptor agonists FTY720 and CYM5442 on atherosclerosis development in LDL receptor deficient (LDL-R^{-/-}) mice. *Vascul. Pharmacol.* **57**, 56–64